PCCP

Polycyclic Aliphatic Hydrocarbons: Is Tetrahedrane Present in UIR Spectra?

Journal:	*Physical Chemistry Chemical Physics*
Manuscript ID	CP-ART-03-2022-001103.R1
Article Type:	Paper
Date Submitted by the Author:	24-May-2022
Complete List of Authors:	Westbrook, Brent; University of Mississippi, Department of Chemistry Beasley, Griffin; Florence High School Fortenberry, Ryan; University of Mississippi, Department of Chemistry & Biochemistry

Journal Name

ARTICLE TYPE

Cite this: DOI: 00.0000/xxxxxxxxxx

Polycyclic Aliphatic Hydrocarbons: Is Tetrahedrane Present in UIR Spectra?†

Brent R. Westbrook,[a] Griffin M. Beasley,[b] and Ryan C. Fortenberry*[a]

Received Date
Accepted Date

DOI: 00.0000/xxxxxxxxxx

The smallest Platonic hydrocarbon, tetrahedrane, has been subject to frequent theoretical and experimental study for 50 years, but its infrared spectrum and synthetic pathway remain a mystery. The recent partial attribution of the ultraviolet extinction bump observed in the interstellar medium (ISM) of the Milky Way galaxy to hydrogenated T-carbon, a larger tetrahedral cluster formed from tetrahedrane and C_4 monomers, has brought renewed interest to the molecule. Similarly, as a polycyclic hydrocarbon, tetrahedrane is similar in structure to the molecules proposed to be responsible for the so-called unidentified infrared bands (UIRs) observed in all kinds of astronomical environments. Furthermore, tetrahedrane's ν_2 and ν_7 fundamental vibrational frequencies, with values of 3210.6 cm^{-1} (3.11 μm) and 752.5 cm^{-1} (13.29 μm) as computed in the present quantum chemical study, have substantial intensities of 59 and 183 km mol^{-1}, respectively. These come tantalizingly close to, but potentially distinct from, the 3.3 and 13.2 μm regions of the infrared spectrum typically included in the UIRs. As such, tetrahedrane or related clusters of these polycyclic aliphatic hydrocarbons may have a role to play in both of these sets of observations and could even help to explain the relation between them. Regardless, if tetrahedrane is present in the ISM, the highly-accurate theoretical data reported herein should help to aid in its identification and may assist in guiding future synthetic experiments as well.

1 Introduction

The unidentified infrared bands (UIRs) are a series of unattributed spectral features found in the infrared range towards virtually all kinds of astronomical objects[1]. They were first recognized in the 8-13 μm region in 1973 around the planetary nebulae NGC 7027, BD+30°3639, and NGC 6572[2], but they have since been observed around hydrogen-rich emission nebulae, post-asymptotic giant branch stars, other planetary nebulae, young stellar objects, in the diffuse interstellar medium (ISM), and in galaxies[1]. Since the original detection, the number of spectral features included under the UIR name has been expanded to include those around 3 μm[3,4] and between 5 and 8 μm[5] with the major groups falling around 3.3, 6.2, 7.7, 8.6, 11.2, 12.7, 13.2, 14.5 and 16.4 μm[1,6,7]. Despite this ubiquity, very little is known about the particular molecules responsible for the spectra. Early hypotheses for their identities pointed to mineral grains composed of molecules like $MgCO_3$[2] and the fluorescence of small molecules on the surface of icy grains[8]. However, since 1984[9,10], polycyclic aromatic hydrocarbons (PAHs) have become the widely-accepted explanation for the majority of the UIR spectral features.

PAHs, as the name indicates, are molecules composed of fused, aromatic rings consisting of carbon and hydrogen atoms. These molecules, as a class, share several characteristics that make them likely carriers of the UIRs. First, even quite large PAHs are still "small species" relative to dust grains and minerals, and such species have the low heat capacity required to emit in the mid-IR even when absorbing a single photon[7]. Second, the extensive π conjugation of PAHs makes them very stable[11], lending credence to their broad ubiquity in the universe. Finally, and arguably most importantly, the few PAHs that have been examined thus far either experimentally or theoretically have spectral profiles that correspond very well to the UIR features[11]. However, in light of more recent evidence and the ever-greater quantity of observational spectra available, the pure PAH hypothesis has been revised to include related molecules like substituted PAHs and aliphatic hydrocarbon structures[12,13]. Such molecules are hypothesized to contribute directly to the UIRs[12,14–18] and may also help to account for the original formation of PAHs, even if PAHs are still responsible for the major spectral features themselves.

Tetrahedrane, as shown in Fig. 1, is a rather exotic example of

[a] Department of Chemistry & Biochemistry, University of Mississippi, University, MS 38677-1848, United States.
[b] Florence High School, Florence, AL 35630, United States.
* E-mail: r410@olemiss.edu

† Electronic Supplementary Information (ESI) available: Type-1 and -2 Fermi resonances and polyads, vibrational frequencies and rotational constants for singly-substituted isotopologues of tetrahedraneSee DOI: 00.0000/00000000.

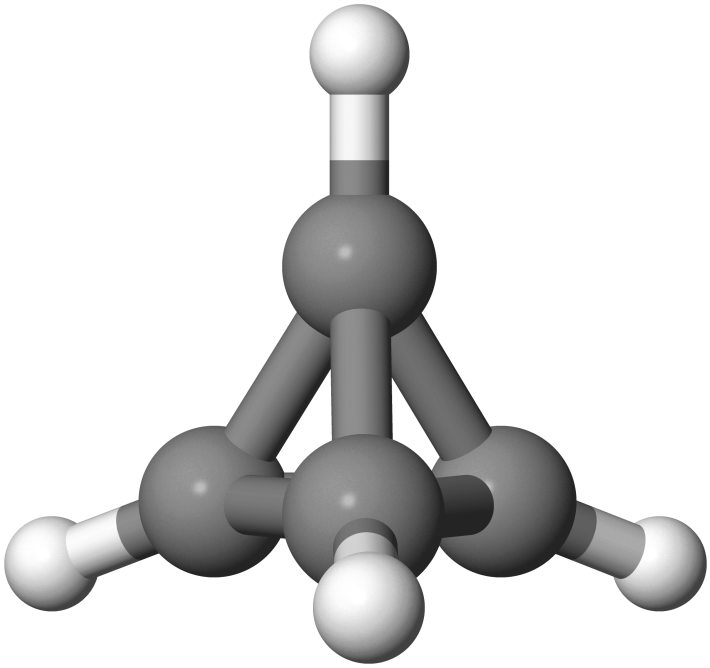

Fig. 1 Visual depiction of tetrahedrane

such an aliphatic hydrocarbon. As the smallest of the Platonic hydrocarbons, tetrahedrane has been the subject of vigorous investigation for more than the past 50 years[19,20]. Despite its obviously high angle strain, it has been shown to be a local minimum on the C_4H_4 potential energy surface[21], 58.7 kcal mol^{-1} above the global minimum of vinlyacetylene. More recently, hydrogenated T-carbon (HTC, $C_{40}H_{16}$), a larger tetrahedron composed of tetrahedral C_4 monomers like tetrahedrane, has been proposed as a contributor to the ultraviolet (UV) extinction bump observed in the interstellar medium (ISM) of the Milky Way[22,23]. Between the hypothesized formation of PAHs from UV processed aliphatic species[12] and this attribution of the UV extinction bump to HTC, the tetrahedrane monomer may have a substantial role to play in these spectral mysteries.

Unfortunately, efforts to synthesize tetrahedrane have thus far been unsuccessful[24], despite the successful synthesis of its Platonic relatives cubane and dodecahedrane[25]. As a result, a plethora of theoretical investigations have sought to predict the spectral features of tetrahedrane[19,20,26,27]. However, because of the substantial size of tetrahedrane, these investigations have been limited to density functionals like BLYP[28,29] or methods like MP2[30] with small basis sets[26,27]. On top of the level of theory, even the most recent of these previous studies relies on scaled harmonic vibrational frequency values rather than explicitly-computed, fundamental anharmonic frequencies[27]. The difficulty of synthesis has likely played a role in the cooling of theoretical interest in tetrahedrane, but with the recent launch of the *James Webb Space Telescope* (JWST) and the aforementioned potential for this molecule to play a role in unidentified spectral features of the ISM, more accurate theoretical data are warranted to examine the role that this molecule may play in astrophysical environments.

To this end, quartic force fields (QFFs) combined with vibrational perturbation theory at second order (VPT2) provide an efficient means of computing highly-accurate theoretical rovibrational spectral data[31]. QFFs are fourth-order Taylor series approximations to the internuclear potential portion of the Watson Hamiltonian[31]. Computing the energies composing the QFF with coupled cluster theory at the perturbative triples level of theory[32] within the F12b explicitly correlated construction[33,34] [CCSD(T)-F12b] and with the corresponding cc-pVTZ-F12 basis sets[35,36] strikes the desired balance between accuracy and computational cost. Such a scheme is often abbreviated as F12-TZ and typically achieves agreement to within 5 to 7 cm^{-1} of gas-phase experimental IR frequencies[37–41]. Contributing to this good agreement is the fact that VPT2 can also account for type-1 and -2 Fermi resonances, Fermi polyads, Coriolis resonances, and Darling-Dennison resonances. Handling these contributions has been shown to be highly important for obtaining accurate spectral data[42,43] and, as such, is one of the strengths of the QFF approach described here.

Nevertheless, QFFs are not entirely without their weaknesses. Most formulations of QFFs rely on the construction of internal coordinate systems, which helps to reduce the cost of the computation[31]. However, these coordinate systems can be difficult to derive uniquely for highly symmetric and cyclic molecules like tetrahedrane. Fortunately, recent work[44] has demonstrated the efficacy of a direct Cartesian QFF for handling such highly symmetric molecules. Thus, the same Cartesian QFF approach is herein applied to tetrahedrane to generate highly accurate fundamental frequencies that can be used by NASA missions such as the ongoing *Stratospheric Observatory for Infrared Astronomy* (SOFIA) and the recently launched JWST to shed some light on new possible carriers of the UIRs. In turn, such data may also help to explain the UV extinction bump and the interplay between these two heretofore unexplained phenomena.

2 Computational Details

The geometry optimization and single point energies composing the QFF are performed at the CCSD(T)-F12b/cc-pVTZ-F12 level of theory[32–35,37,45] within the MOLPRO 2020.1 software package[46]. For these calculations, the one- and two-electron integrals are converged to 1×10^{-22} E_h, the Hartree-Fock energy is converged to 1×10^{-10} E_h, and the CCSD(T)-F12b portion is converged to 1×10^{-8} E_h. The double-harmonic infrared intensities are computed at the MP2/aug-cc-pVDZ level of theory[30,47] using the Gaussian16 program suite[48]. Previous work has shown semi-quantitative accuracy can be achieved in even the harmonic infrared intensities at this level of theory[49–51] for a very low computational cost.

Following the geometry optimization, displacements of 0.005 Å are taken along the Cartesian x, y, and z coordinates to map out the QFF. At each of these 242704 displaced geometries, single-point energies are obtained, and central finite differences of these energies yield the second-, third-, and fourth-order force constants. These force constants are then used by the second-order rotational perturbation theory[52] and VPT2[53,54] implementations in the SPECTRO[55] program. Type-1 and -2 Fermi resonances and polyads, Coriolis resonances, and Darling-Dennison resonances

are handled to increase the accuracy of the resulting anharmonic spectral data[42,43]. In particular, the Type-1 Fermi resonance $2\nu_7 = \nu_3$, and the Type-2 Fermi resonances, $\nu_8 + \nu_6 = \nu_3$ and $\nu_8 + \nu_7 = \nu_4$, are addressed.

3 Results and Discussion

3.1 Vibrational Frequencies

Mode	Symm.	Desc.	Int.	F12-TZ	MP2[a]
ω_1	a_1	symm. C-H stretch	0	3380.2 (2.96)	
ω_2	t_2	anti-symm. C-H stretch	59	3344.1 (2.99)	
ω_3	a_1	breathing	0	1439.2 (6.95)	
ω_4	t_2	anti-symm. C-C stretch	14	1149.0 (8.70)	
ω_5	t_1	H wag	0	888.7 (11.25)	
ω_6	e	C trapezoidal deformation	0	837.2 (11.94)	
ω_7	t_2	H wag	183	774.9 (12.90)	
ω_8	e	H trapezoidal deformation	0	562.6 (17.77)	
ZPVE				12836.7 (0.78)	
ν_1	a_1	symm. C-H stretch		3242.6 (3.08)	3215
ν_2	t_2	anti-symm. C-H stretch		3210.6 (3.11)	3180
ν_3	a_1	breathing		1425.1 (7.02)	1277
ν_4	t_2	anti-symm. C-C stretch		1095.6 (9.13)	1053
ν_5	t_1	H wag		849.7 (11.77)	877
ν_6	e	C trapezoidal deformation		808.1 (12.37)	767
ν_7	t_2	H wag		752.5 (13.29)	758
ν_8	e	H trapezoidal deformation		489.8 (20.42)	564

[a]Scaled harmonic MP2/6-31G* results from Ref. 27

Table 1 F12-TZ harmonic and fundamental frequencies, zero-point vibrational energy (ZPVE, in cm^{-1}), and MP2/aug-cc-pVDZ double-harmonic intensities (in km mol^{-1}) of tetrahedrane. The F12-TZ frequencies are additionally shown in μm in parentheses.

Tetrahedrane's T_d symmetry leaves very few IR-active vibrational modes, as shown in Table 1. Nevertheless, its ν_4 anti-symmetric C-C stretch at 1095.6 cm^{-1} (9.13 μm) has a non-zero, computed double-harmonic intensity of 14 km mol^{-1}. More excitingly, the ν_2 anti-symmetric C-H stretch at 3210.6 cm^{-1} (3.11 μm) has an intensity of 59 km mol^{-1}, which is just below the anti-symmetric stretch of water at about 70 km mol^{-1}. However, the most intense mode, the ν_7 H wag at 752.5 cm^{-1} (13.29 μm), has a very high intensity of 183 km mol^{-1}. Such a large intensity in both of these latter frequencies suggests that tetrahedrane may be observable even in fairly low concentrations. Further, both of these frequencies fall close to, but just outside of, the 3.3 and 13.2 μm spectral features typically attributed to PAHs, suggesting that tetrahedrane or some kind of tetrahedrane-substituted PAH may be contributing to the UIR spectra. If this is the case, the lower intensity ν_4 C-C stretch could help to provide unique identification of tetrahedrane in the ISM or even in a laboratory or combustion environments, where other PAH peaks could overlap with its more prominent vibrational frequencies.

Returning to the high-intensity fundamentals, in the spectra from Orion Bar and NGC7027 reported in[12], a small but distinct peak is present near 3.1 μm, as well as a large peak near 13.3 μm, in the NGC7027 spectrum. These may already offer existing evidence for the astrochemical presence of tetrahedrane, or molecules like it. While larger clusters of tetrahedrane akin to HTC will break the high symmetry and allow for observations of more fundamentals, tetrahedrane is showing that it and potentially related polycyclic aliphatic hydrocarbons show some similarities with PAH IR features as well as some differences. The hydrogen stretches of tetrahedrane are blue-shifted relative to those of modeled PAHs[56], and such differences may enable more of the UIR features to be modeled effectively.

Also shown in Table 1 are the previously-reported MP2/6-31G* scaled harmonic frequency values from[27]. The agreement between the two sets is quite poor, with a mean absolute error of 49.6 cm^{-1} across the eight frequencies and a maximum difference of 148.1 cm^{-1} in ν_3. The one point of agreement is ν_7, which is very fortunate for the MP2 results given that this is by the far the most intense mode. However, the other frequencies all differ by more than 27 cm^{-1}. In relative terms, the closest percent difference is also in ν_7 with an error of 0.73%, but the average unsigned percent error is 5.03%, with huge contributions of 15.14% in ν_8 and 10.39% in ν_3. Without experimental data to support either set of data more conclusively, the substantially greater theoretical rigor of the F12-TZ QFF method reported herein combined with the benchmarked accuracies for this method[37–41] should be taken as evidence for the accuracy of the F12-TZ data. Consequently, this work further shows that explicit treatment of anharmonic frequencies are necessary for even semi-quantitative prediction of IR spectra.

3.2 Rotational Constants and Structural Parameters

	Units	F12-TZ	MP2[a]	BLYP[b]
r_e(C-H)	Å	1.06863	1.073	1.074
r_0(C-H)	Å	1.06592		
r_e(C-C)	Å	1.47752	1.477	1.490
r_0(C-C)	Å	1.48578		
$\angle_e$(H-C-C)	°	144.696		144.7
$\angle_0$(H-C-C)	°	144.681		

[a]MP2/6-31G* results from Ref. 27
[b]BLYP/6-311G(2d,2p) results from Ref. 26

Table 2 F12-TZ structural parameters of tetrahedrane

The equilibrium ($_e$) and vibrationally-averaged ($_0$) geometrical parameters for tetrahedrane are given in Table 2, alongside the MP2/6-31G* and BLYP/6-311G(2d,2p) values from[27] and[26], respectively. The MP2 and BLYP results agree well with each other for the equilibrium C-H bond length with values of 1.073 and 1.074 Å, but they both seem to overestimate this distance slightly relative to F12-TZ, which reports a value of 1.06863 Å. In contrast, F12-TZ and MP2 agree well on the C-C bond length at a value of around 1.477 Å, while the BLYP value is substantially higher at 1.490 Å. Only Ref. 26 reports a value for the H-C-C bond angle, but it agrees well with the F12-TZ value of 144.686 degrees determined herein. Overall, both MP2 and BLYP perform fairly well on the structural parameters relative to each other and relative to F12-TZ, but in light of the existing differences, the F12-TZ results should still be the most accurate values available.

The T_d symmetry of tetrahedrane means that it will not have a permanent dipole moment and thus will not be observable by pure rotational spectroscopy. Regardless, the equilibrium, vibrationally-averaged, and singly-vibrationally-excited principal

Const.	Units	Value
B_e	MHz	13773.7
B_0	MHz	13667.3
B_1	MHz	13641.2
B_2	MHz	13645.2
B_3	MHz	13638.3
B_4	MHz	13680.5
B_5	MHz	13764.1
B_6	MHz	13663.7
B_7	MHz	13732.0
B_8	MHz	13644.5
Δ_J	kHz	7.678
Δ_K	kHz	−2.974
Δ_{JK}	kHz	3.263
δ_J	Hz	115.523
δ_K	kHz	−1.561
Φ_J	mHz	5.934
Φ_K	mHz	531.329
Φ_{JK}	mHz	163.929
Φ_{KJ}	mHz	−639.634
ϕ_j	mHz	1.502
ϕ_{jk}	mHz	−94.420
ϕ_k	mHz	255.286

Table 3 F12-TZ rotational constants of tetrahedrane

rotational constants for tetrahedrane are reported in Table 3 along with the quartic and sextic distortion coefficients. Additionally, the B_2 and B_7 constants will be particularly useful for modeling the rovibrational spectra of the most intense anharmonic frequencies. Despite the lack of rotational activity in the ground vibrational state and in five of the eight fundamental frequencies, these spectroscopic constants may still be helpful for accurate thermochemical analysis or kinetic rate determination that require the full rotational partition function.

3.3 Singly-Substituted Isotopologues

The vibrational frequencies and rotational constants for the singly-deuterated and singly-^{13}C-substituted isotopologues are reported in Tables S1 and S2 of the Electronic Supplementary Information (ESI). Both of these substitutions break the T_d symmetry of the molecule and lead the formerly-degenerate e and t_2 modes to split. As expected, the deuterium substitution substantially decreases the frequency of the C-H stretches, especially in the case of ν_4, which splits from the relabeled ν_2 and ν_3 by more than 800 cm^{-1}. The ^{13}C substitution has less of an effect on these frequencies, with ν_2, ν_3, and ν_4 still nearly degenerate, separated at most by 20 cm^{-1}. Similarly, the deuterium substitution causes more differences to arise in the H wags and deformations, while the ^{13}C has a greater effect on the C-C stretch and deformation. Both substitutions dampen the breathing mode, redshifting it to 1378.4 cm^{-1} (7.25 μm) for the deuterium and to 1390.4 cm^{-1} (7.19 μm) for the ^{13}C.

The symmetry breaking of these isotopic substitutions also introduces small, but non-zero dipole moments, as shown in Table S2 of the ESI. In the case of the deuterium substitution, the Born-Oppenheimer dipole moment is computed to be 0.2 D. That of the ^{13}C isotopologue is less than 0.1 D. While these are quite small, they may still enable the rotational observation of these molecules, and the relative abundance of D and ^{13}C should make these substitutions possible, if tetrahedrane itself can form. The decrease in symmetry for the isotopologues also splits the A and C rotational constants in both cases, but the separation is more pronounced in the case of D, with a difference between A_0 and C_0 of 1296.6 MHz, compared to only 311.6 MHz for ^{13}C. In both cases, the A_0 values remain close to the B_0 value for non-substituted tetrahedrane at 13667.3 MHz, while the C_0 value is farther away, as is expected for near-oblate molecules.

4 Conclusions

This work provides the most accurate theoretical rovibrational spectral data available for the tetrahedrane molecule. Despite 50 years of active investigation, this molecule has yet to be conclusively synthesized in the laboratory, and the data provided herein should help to identify it, if it can be experimentally generated. Furthermore, tetrahedrane is a monomer of HTC, a form of carbon recently proposed to be partially responsible for the UV extinction bump in the ISM, suggesting tetrahedrane itself may likely be found there as well. Tetrahedrane is also a polycyclic aliphatic hydrocarbon with two of its eight fundamental vibrational frequencies found very close to the UIR spectral features at 3.3 and 13.2 μm. In particular, its ν_2 anti-symmetric C-H stretch at 3210.6 cm^{-1} (3.11 μm) has a fairly high intensity of 59 km mol^{-1} and its ν_7 H wag at 752.5 cm^{-1} (13.29 μm) has an even greater intensity of 183 km mol^{-1}. Given these two intense frequencies, if tetrahedrane is present in the ISM, it should be observable by NASA missions operating in the IR region of the spectrum like the recently-launched JWST and the ongoing SOFIA mission. Such an observation would likely shed light not only on the carriers of the UIRs, but also on the cause of the UV extinction bump and how these two processes are interrelated. Finally, and more broadly, tetrahedrane represents the simplest form of HTC that could be a competitor with PAHs for carbon abundance and IR emission spectra. This work shows that while tetrahedrane, and HTCs by extension, share many similarities with presumed PAH features, they exhibit a few notable differences that may help to flesh out more completely the structure of the UIRs.

Author Contributions

Conceptualization: RCF; Data curation: BRW, GMB; Formal Analysis: BRW; Funding acquisition: RCF; Investigation: GMB, BRW; Methodology: RCF, BRW; Project administration: RCF; Resources: RCF; Software: BRW, RCF; Supervision: RCF, BRW; Validation: BRW, RCF; Visualization: BRW; Writing – original draft: BRW, RCF; Writing – review & editing: RCF, BRW, GMB;

Conflicts of interest

There are no conflicts to declare.

Acknowledgements

This work is supported by NASA Grant NNX17AH15G and NSF Grant OIA-1757220. The Mississippi Center for Supercomputing Research (MCSR) is thanked for its gracious provision of compu-

tational resources.

Notes and references

1 E. Peeters, S. Hony, C. Van Kerckhoven, A. G. G. M. Tielens, L. J. Allamandola, D. M. Hudgins and C. W. Bauschlicher, *Astron. Astrophys.*, 2002, **390**, 1089–1113.

2 F. C. Gillett, W. J. Forrest and K. M. Merrill, *Astrophys. J.*, 1973, **183**, 87–93.

3 R. W. Russell, B. T. Soifer and W. J. Forrest, *Astrophys. J.*, 1975, **198**, L41–L43.

4 T. R. Geballe, J. H. Lacy, S. E. Persson, P. J. McGregor and B. T. Soifer, *Astrophys. J.*, 1985, **292**, 500–505.

5 M. Cohen, L. Allamandola, A. G. G. M. Tielens, J. Bregman, J. P. Simpson, F. C. Witteborn, D. Wooden and D. Rank, *Astrophys. J.*, 1986, **302**, 737–749.

6 E. Peeters, L. J. Allamandola, D. M. Hudgins, S. Hony and A. G. G. M. Tielens, *Astrophysics of Dust, ASP Conference Series*, Astronomical Society of the Pacific, San Francisco, CA, 2004, vol. 309, pp. 141–162.

7 A. G. G. M. Tielens, *Annu. Rev. Astron. Astrophys.*, 2008, **46**, 289–337.

8 L. J. Allamandola, J. M. Greenberg and C. A. Norman, *Astron. Astrophys.*, 1979, **77**, 66–74.

9 K. Sellgren, *Astrophys. J.*, 1984, **277**, 623–633.

10 A. Leger and J. L. Puget, *Astron. Astrophys.*, 1984, **137**, L5–L8.

11 L. J. Allamandola, A. G. G. M. Tielens and J. R. Barker, *Astrophys. J. Suppl. Ser.*, 1989, **71**, 733–775.

12 E. Peeters, *Proc. Int. Astron. Union*, 2011, **7**, 149–161.

13 A. G. G. M. Tielens, in *25 Years of PAH Hypothesis*, EDP Sciences, 2021, pp. 1–10.

14 G. C. Sloan, M. Jura, W. W. Duley, K. E. Kraemer, J. Bernard-Salas, W. J. Forrest, B. Sargent, A. Li, D. J. Barry, C. J. Bohac, D. M. Watson, and J. R. Houck, *Astrophys. J.*, 2007, **664**, 1144–1153.

15 C. Boersma, J. Bouwman, F. Lahus, C. van Kerckhoven, A. G. G. M. Tielens, L. B. F. M. Waters and T. Henning, *Astron. Astrophys.*, 2008, **484**, 241–249.

16 L. D. Keller, G. C. Sloan, W. J. Forrest, S. Ayala, P. D'Alessio, S. Shah, N. Calvet, J. Najita, A. Li, L. Hartmann, B. Sargent, D. M. Watson and C. H. Chen, *Astrophys. J.*, 2008, **684**, 411–429.

17 T. Pino, E. Dartois, A.-T. Cao, Y. Carpentier, T. Chamaillé, R. Vasquez, A. P. Jones, L. d'Hendecourt and P. Bréchignac, *Astron. Astrophys.*, 2008, **490**, 665–672.

18 B. Acke, J. Bouwman, A. Juhász, T. Henning, M. E. van den Ancker, G. Meeus, A. G. G. M. Tielens and L. B. F. M. Waters, *Astrophys. J.*, 2010, **718**, 558–574.

19 J. M. Schulman and T. J. Venanzi, *J. Am. Chem. Soc.*, 1974, **96**, 4739–4746.

20 N. S. Zefirov, A. S. Koz'min and A. V. Abramenkov, *Russ. Chem. Rev.*, 1978, **47**, 163–171.

21 A. M. Mebel, V. V. Kislov and R. I. Kaiser, *J. Chem. Phys.*, 2006, **125**, 133113.

22 T. P. Stecher, *Astrophys. J.*, 1965, **142**, 1683–1684.

23 X.-Y. Ma, Y.-Y. Zhu, Q.-B. Yan, J.-Y. You and G. Su, *Mon. Not. Royal Astron. Soc.*, 2020, **497**, 2190–2200.

24 Y. Kobayashi, M. Nakamoto, Y. Inagaki and A. Sekiguchi, *Angew. Chem. Int. Ed.*, 2013, **52**, 10740–10744.

25 A. Nemirowski, H. P. Reisenauer and P. R. Schreiner, *Chem. Eur. J.*, 2006, **12**, 7411–7420.

26 B. S. Jursic, *J. Mol. Structure (THEOCHEM)*, 2000, **507**, 185–192.

27 L. S. Karpushenkava, G. J. Kabo and A. B. Bazyleva, *J. Mol. Structure (THEOCHEM)*, 2009, **913**, 43–49.

28 A. D. Becke, *Phys. Rev. A*, 1988, **38**, 3098–3100.

29 C. Lee, W. T. Yang and R. G. Parr, *Phys. Rev. B.*, 1988, **37**, 785–789.

30 C. Møller and M. S. Plesset, *Phys. Rev.*, 1934, **46**, 618–622.

31 R. C. Fortenberry and T. J. Lee, *Ann. Rep. Comput. Chem.*, 2019, **15**, 173–202.

32 K. Raghavachari, G. W. Trucks, J. A. Pople and M. Head-Gordon, *Chem. Phys. Lett.*, 1989, **157**, 479–483.

33 T. B. Adler, G. Knizia and H.-J. Werner, *J. Chem. Phys.*, 2007, **127**, 221106.

34 G. Knizia, T. B. Adler and H.-J. Werner, *J. Chem. Phys.*, 2009, **130**, 054104.

35 K. A. Peterson, T. B. Adler and H.-J. Werner, *J. Chem. Phys.*, 2008, **128**, 084102.

36 K. E. Yousaf and K. A. Peterson, *J. Chem. Phys.*, 2008, **129**, 184108.

37 X. Huang, E. F. Valeev and T. J. Lee, *J. Chem. Phys.*, 2010, **133**, 244108.

38 D. Agbaglo, T. J. Lee, R. Thackston and R. C. Fortenberry, *Astrophys. J.*, 2019, **871**, 236.

39 D. Agbaglo and R. C. Fortenberry, *Int. J. Quantum Chem.*, 2019, **119**, e25899.

40 D. Agbaglo and R. C. Fortenberry, *Chem. Phys. Lett.*, 2019, **734**, 136720.

41 B. R. Westbrook and R. C. Fortenberry, *J. Phys. Chem. A*, 2020, **124**, 3191–3204.

42 J. M. L. Martin, T. J. Lee, P. R. Taylor and J.-P. François, *J. Chem. Phys.*, 1995, **103**, 2589–2602.

43 J. M. L. Martin and P. R. Taylor, *Spectrochim. Acta A*, 1997, **53**, 1039–1050.

44 B. R. Westbrook, E. M. Valencia, S. C. Rushing, G. S. Tschumper and R. C. Fortenberry, *J. Chem. Phys.*, 2021, **154**, 041104.

45 J. G. Hill, S. Mazumder and K. A. Peterson, *J. Chem. Phys.*, 2010, **132**, 054108.

46 H.-J. Werner, P. J. Knowles, F. R. Manby, J. A. Black, K. Doll, A. Heßelmann, D. Kats, A. Köhn, T. Korona, D. A. Kreplin, Q. Ma, T. F. Miller, A. Mitrushchenkov, K. A. Peterson, I. Polyak, G. Rauhut and M. Sibaev, *WIREs Comput. Mol. Sci.*, 2020.

47 R. A. Kendall, T. H. Dunning and R. J. Harrison, *J. Chem. Phys.*, 1992, **96**, 6796–6806.

48 M. J. Frisch, G. W. Trucks, H. B. Schlegel, G. E. Scuseria, M. A. Robb, J. R. Cheeseman, G. Scalmani, V. Barone, G. A. Peters-

son, H. Nakatsuji, X. Li, M. Caricato, A. V. Marenich, J. Bloino, B. G. Janesko, R. Gomperts, B. Mennucci, H. P. Hratchian, J. V. Ortiz, A. F. Izmaylov, J. L. Sonnenberg, D. Williams-Young, F. Ding, F. Lipparini, F. Egidi, J. Goings, B. Peng, A. Petrone, T. Henderson, D. Ranasinghe, V. G. Zakrzewski, J. Gao, N. Rega, G. Zheng, W. Liang, M. Hada, M. Ehara, K. Toyota, R. Fukuda, J. Hasegawa, M. Ishida, T. Nakajima, Y. Honda, O. Kitao, H. Nakai, T. Vreven, K. Throssell, J. A. Montgomery, Jr., J. E. Peralta, F. Ogliaro, M. J. Bearpark, J. J. Heyd, E. N. Brothers, K. N. Kudin, V. N. Staroverov, T. A. Keith, R. Kobayashi, J. Normand, K. Raghavachari, A. P. Rendell, J. C. Burant, S. S. Iyengar, J. Tomasi, M. Cossi, J. M. Millam, M. Klene, C. Adamo, R. Cammi, J. W. Ochterski, R. L. Martin, K. Morokuma, O. Farkas, J. B. Foresman and D. J. Fox, *Gaussian 16 Revision C.01*, 2016, Gaussian Inc. Wallingford CT.

49 Q. Yu, J. M. Bowman, R. C. Fortenberry, J. S. Mancini, T. J. Lee, T. D. Crawford, W. Klemperer and J. S. Francisco, *J. Phys. Chem. A*, 2015, **119**, 11623–11631.

50 B. Finney, R. C. Fortenberry, J. S. Francisco and K. A. Peterson, *J. Chem. Phys.*, 2016, **145**, 124311.

51 B. R. Westbrook, D. J. Patel, J. D. Dallas, G. C. Swartzfager, T. J. Lee and R. C. Fortenberry, *J. Phys. Chem. A*, 2021, **125**, 8860–8868.

52 I. M. Mills, *Molecular Spectroscopy - Modern Research*, Academic Press, New York, 1972, pp. 115–140.

53 J. K. G. Watson, *Vibrational Spectra and Structure*, Elsevier, Amsterdam, 1977, pp. 1–89.

54 D. Papousek and M. R. Aliev, *Molecular Vibration-Rotation Spectra*, Elsevier, Amsterdam, 1982.

55 J. F. Gaw, A. Willets, W. H. Green and N. C. Handy, 1996, *SPECTRO program*, version 3.0.

56 C. W. Bauschlicher, Jr., A. Ricca, C. Boersma and L. J. Allamandola, *Astrophys. J. Suppl. Ser.*, 2018, **234**, 32.